Heliyon 6 (2020) e04355

Contents lists available at ScienceDirect

Heliyon

journal homepage: www.cell.com/heliyon

Research article

Global warming leading to alarming recession of the Arctic sea-ice cover: Insights from remote sensing observations and model reanalysis

Avinash Kumar *, Juhi Yadav, Rahul Mohan

National Centre for Polar and Ocean Research (NCPOR), Ministry of Earth Science, Government of India, Vasco-da-Gama, Goa, India

ARTICLE INFO

Keywords:
Atmospheric science
Environmental science
Earth sciences
Natural hazards
Oceanography
Arctic sea-ice
Global temperature
Sea-ice thickness
Multiyear ice
Climate change

ABSTRACT

The present study quantifies the magnitude of Arctic sea-ice loss in the boreal summer (July–September), especially in September at different timescales (daily, monthly, annual and decadal). The investigation on the accelerated decline in the Arctic sea-ice was performed using different datasets of passive microwave satellite imagery and model reanalysis. Arctic sea-ice declined rapidly in the boreal summer (-10.2 ± 0.8 %decade^{-1}) during 1979–2018, while, the highest decline in sea-ice extent (SIE) (i.e., 82,300 km^2 yr^{-1}/-12.8 ± 1.1 %decade^{-1}) is reported in the month of September. Since late 1979, the SIE recorded the sixth-lowest decline during September 2018 (4.71 million km^2). Incidentally, the records of twelve lowest extents in the satellite era occurred in the last twelve years. The loss of SIE and sea-ice concentration (SIC) are attributed to the impacts of land-ocean warming and the northward heat advection into the Arctic Ocean. This has resulted in considerable thinning of sea-ice thickness (SIT) and reduction in the multiyear ice (MYI) for summer 2018. Global and Arctic land-ocean temperatures have increased by ~0.78 °C and ~3.1 °C, respectively, over the past 40 years (1979–2018) while substantial warming rates have been identified in the Arctic Ocean (~3.5 °C in the last 40-year) relative to the Arctic land (~2.8 °C in the last 40-year). The prevailing ocean-atmospheric warming in the Arctic, the SIE, SIC and SIT have reduced, resulting in the decline of the sea-ice volume (SIV) at the rate of -3.0 ± 0.2 (1000 km^3 decade^{-1}). Further, it observed that the SIV in September 2018 was three times lower than September 1979. The present study demonstrates the linkages of sea-ice dynamics to ice drifting and accelerated melting due to persistent low pressure, high air-ocean temperatures, supplemented by the coupled ocean-atmospheric forcing.

1. Introduction

Seasonal changes in the Arctic sea-ice plays a crucial role in regulating the global climate [1]. Arctic sea-ice occupies a land-locked ocean region that stretches all the way to the north pole with the highest sea-ice extent (SIE) oscillations occurring between winter and summer months. SIE in the Northern Hemisphere shows negative trends for all the months (Figure 1) with the maximum SIE reported in March and minimum in September [2]. Over the past four decades, the SIE variability in late winter ranged from about 14-16 million km^2, whereas in each September the extent reaches about 7 million km^2 [3, 4].

In recent decades, the historic retreat of Arctic SIE, especially during summer [5, 6] has been driven by the following factors - (i) absorption of more solar energy by open water [7, 8, 9]; (ii) strong southerly winds advecting warm temperatures [10, 11]; (iii) a strengthened wind-driven transpolar drift causing huge amounts of ice to either exit the Arctic Ocean through Fram Strait or pile up at the edge of the Canadian Arctic Archipelago basin [12, 13], and (iv) downward energy fluxes from the atmosphere and northward ocean heat transport [14, 15, 16].

Arctic sea-ice melting has accelerated with a reduced surface albedo due to a resultant increase in the absorption of solar radiation, by the darker ocean surface. This positive feedback process amplifies Arctic air temperatures [3]. Warming processes in the Arctic is faster than the rest of the globe during the last few decades [17]. During the boreal summer negative phase index of Arctic oscillation (AO) condition supports south-easterly wind anomalies which enhances advection of ice, away from the Alaskan coast. This also enhances the advection of warm air onto the ocean thereby decreasing the amount of ice in the Beaufort and Chukchi seas [18]. However, in the years of low SIE during September, it is characterized by anticyclonic circulation disturbances over the Arctic Ocean [19].

Arctic SIE has reported critically lowest value in the last decade, especially during September 2012 (3.57 million km^2) with the advent of satellite sea-ice observations beginning in the 1970s (Figures 1 and 2).

* Corresponding author.
E-mail addresses: avinash@ncpor.res.in, kumaravinash13@gmail.com (A. Kumar).

https://doi.org/10.1016/j.heliyon.2020.e04355
Received 22 December 2019; Received in revised form 16 March 2020; Accepted 24 June 2020

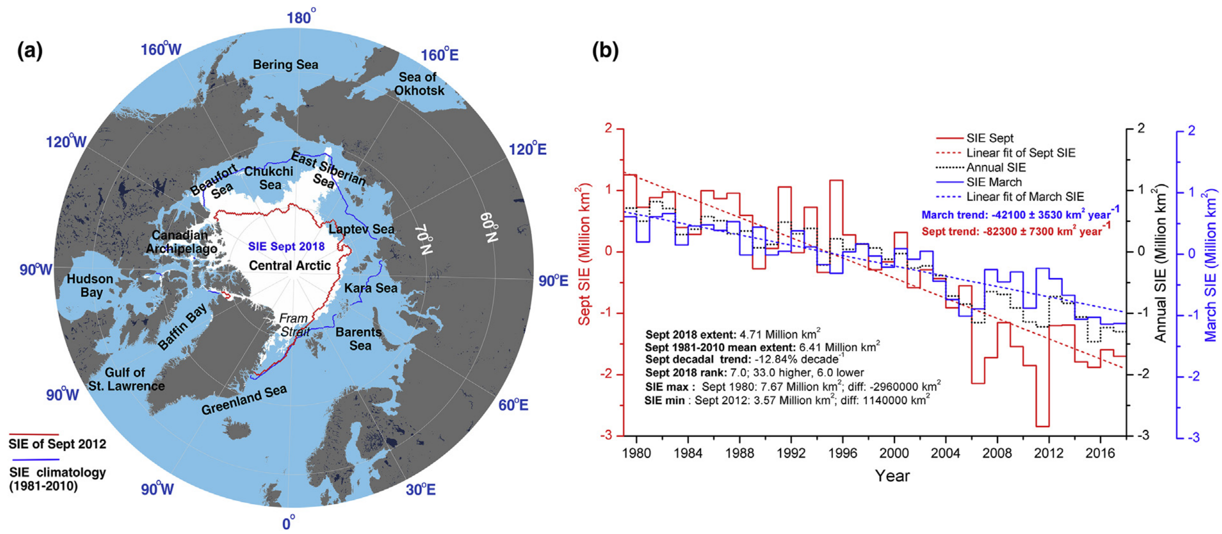

Figure 1. (a) Multisensor analyzed sea ice extent (MASIE) of the Northern Hemisphere showing SIE of September 2018 and their regional seas. The red and dark blue lines delineating SIE of September 2012 and climatology (1979–2010). (b) The time series plot represents SIE anomaly (1979–2018) for March and September with a linear least-squares fit and annual SIE.

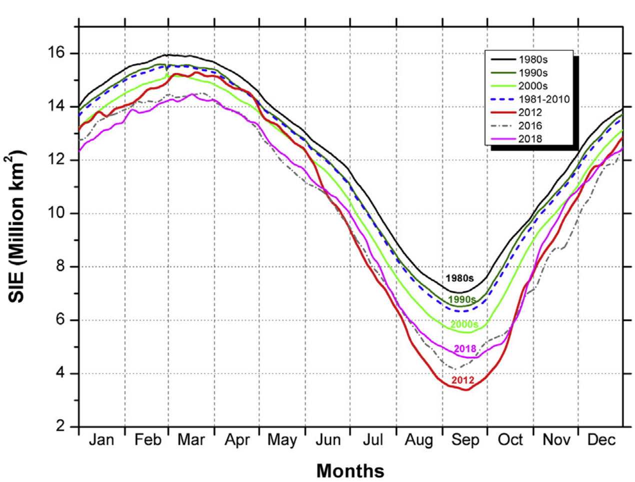

Figure 2. The daily SIE (million km^2) from January to December for the 1980s (1980–1989), 1990s (1990–1999) and 2000s (2000–2009) using black, dark green, light green lines, respectively. Daily SIE has been shown for the year 2012 (red line) with the lowest SIE, followed by 2016 (grey dash-dotted line) and 2018 (pink line). The 1981 to 2010 median shown in the dash blue line. (Daily data obtained from NSIDC).

The lowest SIE record in the summer period occurred at a time of substantial warming in the Arctic. However, since the late 1979 (satellite era), the SIE [20, 21], SIT [22, 23], MYI [8], and SIV [3, 16] have declined dramatically which is an indicator of ongoing climate change [24]. However, the internal climate variability for September Arctic SIE trends is not consistent, as it can either mask or intensify human-induced changes over a decade [25].

Since the 1970s, Arctic sea-ice decline has been reported throughout the year, but significant declines in SIE and SIC have been observed every year in September (Figure 1). The study focuses on the boreal summer months from July to September as this timeframe captures significant signals of diminishing sea-ice. The objective of this study is to investigate the changes in the pan-Arctic sea ice during the boreal summer, especially in September on different timescales (daily, monthly annual and decadal). The study reveals how the ocean-atmospheric forcing is accelerating the sea-ice decline in September 2018. Further, we examine how the high-latitude atmospheric circulation in summertime impacts September SIE. To gain insights into the dramatic decline in summer SIE in 2018, the influence of air temperature, surface temperatures and sea-level pressure is studied to assess the impact on the sea-ice concentration (SIC), sea-ice thickness (SIT), sea-ice volume (SIV) and multiyear ice (MYI) coverage.

2. Materials and methods

Daily and monthly (1979–2018) gridded SIE and SIC data developed by the NASA team from brightness temperature data, based on the following sensors: Nimbus-7 SMMR (1979–1987), DMSP- F8 SSM/I (1987–1991), DMSP-F11 SSM/I (1991–1995), DMSP-F13 SSM/I (1995–2007), DMSP-F13 SSMIS (2008-present) in polar stereographic projection (at 25 $\times$ 25 km spatial resolution) were acquired from the National Snow and Ice Data Center (NSIDC), Colorado [26, 27]. The SIE is derived by summing up the areas of all pixels having at least 15% of SIC of Arctic regions [28].

Air temperature (AT) at 925 hPa, surface temperature (ST), and sea level pressure (SLP) mean and anomaly values related to 1981–2010 climatology reanalysis derived data acquired with a spatial resolution of $1^\circ \times 1^\circ$ from the National Centers for Environmental Prediction/National Center for Atmospheric Research (NCEP/NCAR) and provided by the NOAA/OAR/ESRL PSD, Boulder, Colorado, USA, were available at https://www.esrl.noaa.gov/psd/ [29]. The AT at 925 hPa level provides a better indication of lower tropospheric temperatures than does the 2 m temperature, which is significantly influenced by surface processes and parameterizations in the atmospheric model [30].

We computed the averages for SIE, SIC, temperature, and SLP from the daily and monthly data. Time series of all the anomalies are calculated by removing the climatological monthly means for the period 1981–2010 climatology [31]. Using a least square method, the timeseries data are fitted with a linear function to model the trend. Statistical analyses of NCEP/NCAR reanalysis derived data were processed using Climate Data Operator (CDO) and MATLAB for computation of anomaly from monthly NetCDF files of AT (°C), ST (°C) and SLP (mb). Spatial plots were prepared using the NCAR Command Language (Version 6.6.2) software (https://doi.org/10.5065/D6WD3XH5). Monthly ranking Air temperature map (1979–2018 period) of the Artic region (70° N+) were prepared using Matplotlib in Python v3.5, and the data were available at http://www.esrl.noaa.gov/psd/data/timeseries/. Time series data of temperature anomalies (°C) of land and ocean, based on NCEP R1 data were plotted using the statistical SigmaPlot V.14 Software.

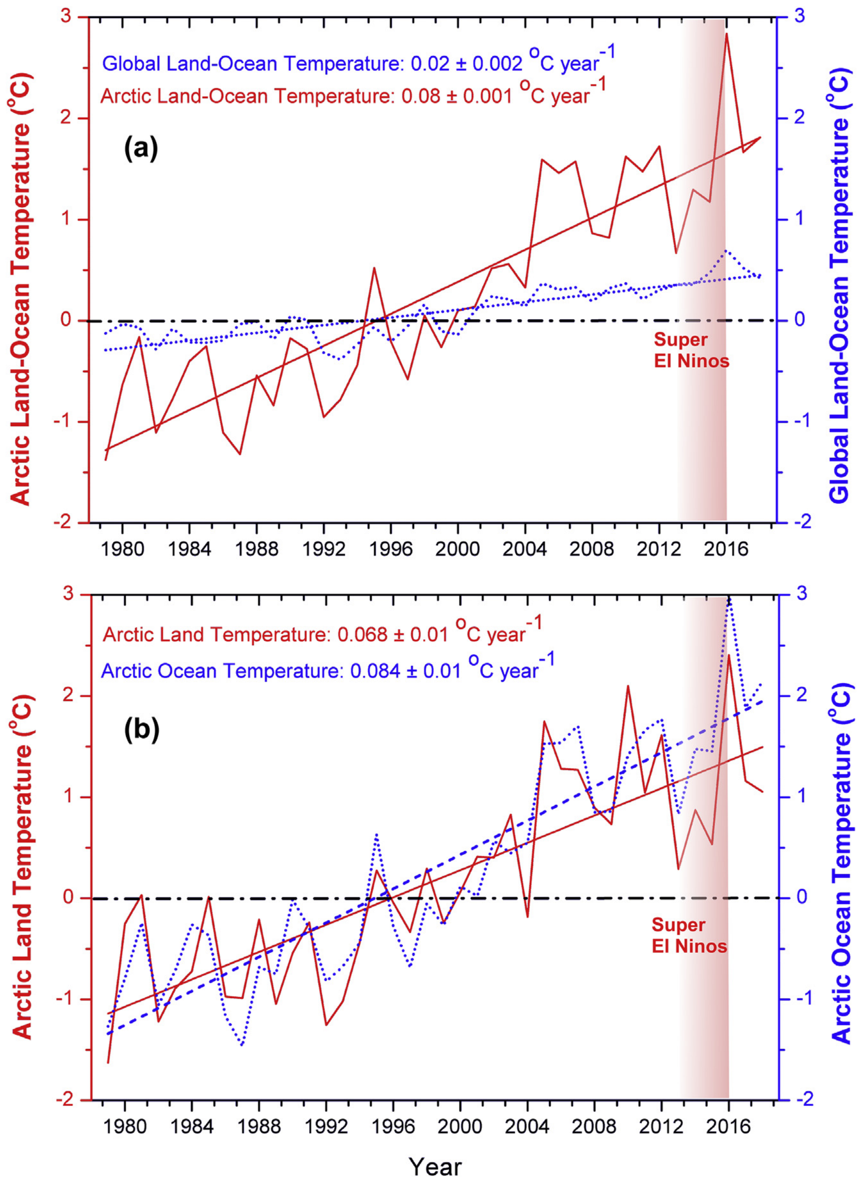

Figure 3. Temperature annual anomalies (°C) of land and ocean (relative to 1981–2010), based on NCEP R1 data for global (90° S to +90° N), Arctic (+70° N) regions during 1979–2018 period. (a) Showing increasing trend of Arctic temperature (in red line) which is significantly higher compared to the global temperature (in dotted blue line); (b) the temperature data computed for Arctic land (red line) and Arctic ocean (blue line) shows since the last decade, Arctic ocean is warming higher compared to the Arctic land. The overall global and Arctic land-ocean warming recorded since the year 2000 whereas super El- Niño event during 2014–2016 is demonstrating accelerated ocean warming effect (red increasing shades).

TOPAZ4 reanalysis data for SIT variables are obtained from Copernicus Marine Environment Monitoring Service (http://marine.copernicus.eu/services-portfolio/access-to-products/?option=com_csw&view=details&product_id=ARCTIC_ANALYSIS_FORECAST_PHYS_002_001_a) for September 2018, with a spatial resolution of 12.5 km × 12.5 km. TOPAZ4 is a coupled ocean-sea ice data assimilation system (based on satellite and in situ observations) for the North Atlantic Ocean and Arctic based on the Hybrid Coordinate Ocean Model (HYCOM) developed at the University of Miami [32], and the ensemble Kalman filter (EnKF) data assimilation [33]. HYCOM uses 28 hybrid layers in the vertical (z-isopycnal) and model's native grid covers the Arctic and North Atlantic Oceans which has fairly homogeneous horizontal spacing (between 11 and 16 km). It provides an accurate estimate of the ocean circulation in the North Atlantic and the sea-ice variability in the Arctic.

Arctic Ocean sea-ice age data derived through remotely sensed sea ice motion and sea ice extent is obtained from the EASE-Grid Sea Ice Age, V.4 (https://nsidc.org/data/NSIDC-0611/versions/4). The sea-ice age product is available in NetCDF format from January 1984 to December 2018 [34]. In this dataset, the method used to compute sea ice age is estimated by treating each grid cell that contains ice as a discrete, independent Lagrangian parcel and tracking the parcels at weekly time-steps advected by the weekly ice motions [8, 34]. The ice age is discretized in annual increments, where a year described as the melting season varying from the minimum Arctic ice extent (above 15% SIC) of one season (usually in September) to the end of the next year. The multiyear sea ice age is considered as first-year ice (0–1 years old), second-year ice (1–2 years old), and so forth based on how many melt seasons the sea ice survives [35]. Multiyear ice (MYI) timeseries and spatial plots were prepared using SigmaPlot V.14 Software and the NCAR Command Language (Version 6.6.2) software (https://doi.org/10.5065/D6WD3XH5), respectively.

SIV (10^3 km^3) is estimated using the Pan-Arctic Ice Ocean Modeling and Assimilation System (PIOMAS V.2.1; http://psc.apl.uw.edu/research/projects/arctic-sea-ice-volume-anomaly/data/) developed at APL/PSC [36]. PIOMAS is a computational model of sea ice and ocean elements and can assimilate empirical data (SIC and sea surface temperature). PIOMAS model grid datasets include a model output for 1978-present and provides with estimates of volume from the satellite-derived sea ice extent data [37]. In this study, monthly SIV data were obtained in ASCII table format with columns for each month and

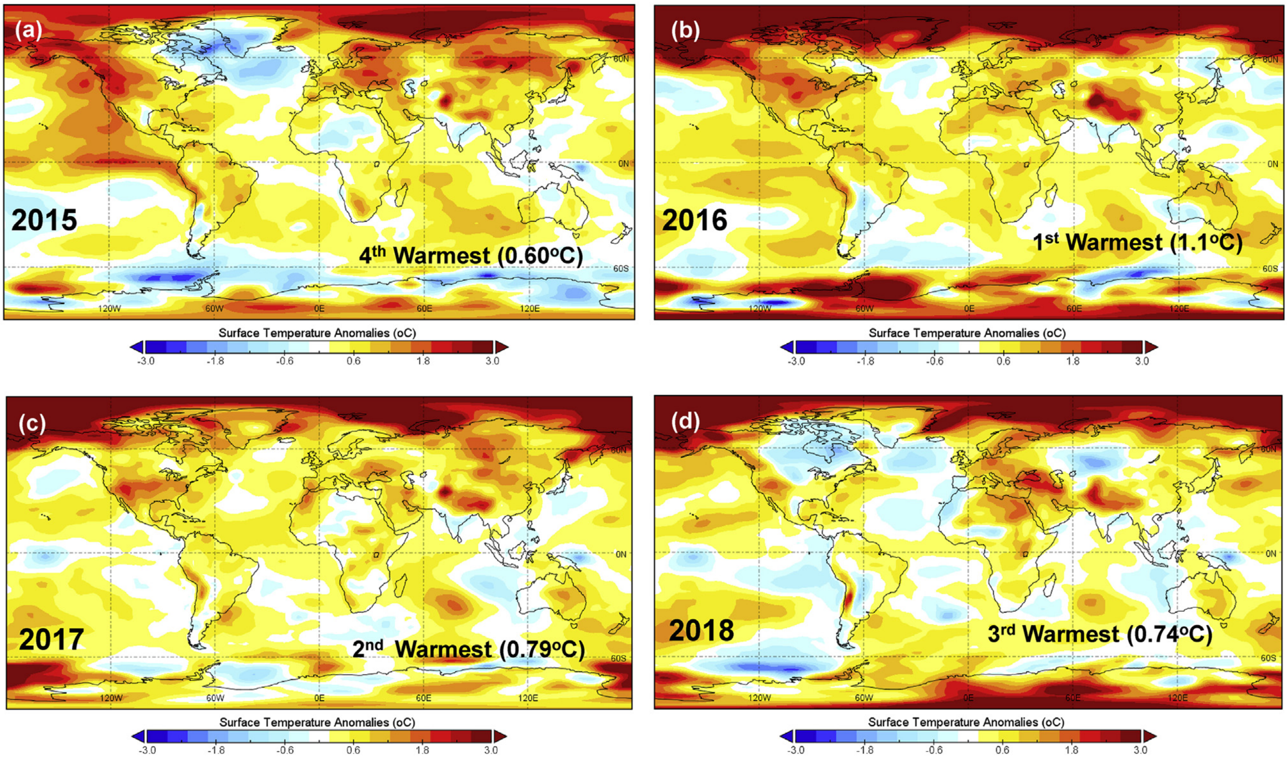

Figure 4. Annual average surface temperature anomalies for the years 2015–2018 relative to the climatology year (1981–2010). The figure shows the super El Niño (2015–16) in the equatorial Pacific Ocean and as its impact, the warmest year was recorded in the year 2016, when the effect of El Niño on global warming was highest.

rows for years 1979–2018. SIV anomalies were calculated by removing the climatological monthly means for the period 1981–2010 and plotted using the SigmaPlot V.14 Software.

3. Results

3.1. Arctic sea-ice melting records in 2018

Available satellite records since 1979, indicated that Arctic SIE reached it's record lows in 2018 January (13.06 million km^2) and February (13.95 million km^2), and remained at the second-lowest from March (14.3 million km^2) to May (12.21 million km^2) (Figure 2), whereas, the SIE reduction is influenced by accelerated sea ice loss in the Bering Sea due to extremely low sea ice extent in the last four decades. However, sea-ice melting started gradually over most of the western Arctic Ocean and the East Siberian Sea [38]. The rate of sea-ice melting in June (~53,000 km^2 day^{-1}) was below the climatology (1981–2010) average (~56,000 km^2 day^{-1}). The SIE of July 2018 has declined at the rate of ~105,500 km^2 day^{-1} which is quite higher than the climatology (i.e., ~89,000 km^2 day^{-1}) (Figure 2), whereas, sea-ice loss in August (~57,500 km^2 day^{-1}) was close to the climatology.

The Arctic SIE was maximum in September 1980 (7.67 million km^2) and minimum in September 2012 (3.57 million km^2), whereas, SIE in September 2018 reduced to 4.71 million km^2, which is 1.70 million km^2 below to the climatology average (6.41 million km^2) (Figures 1 and 2). The sea-ice decline shown in linear rate for September is 82,300 km^2 yr^{-1} (12.8 ± 1.1% decade^{-1}) relative to 1981–2010 average (Figure 1b). The seasonal SIE of 2018 recorded minimum between September 19 and 23. Prior to September 19, 2018, SIE had declined at a rate of ~14,000 km^2 day^{-1} which was significantly faster than in most years, and no sea-ice loss is recorded between September 19 and 23. After September 23, 2018, the onset of significant seasonal ice growth occurred in the Canadian Archipelago, the northern Chukchi and Beaufort Seas, and the East Greenland Sea, while the retreat occurred within the Kara Sea very late, relative to the satellite era (Figure 1a). The sea-ice retreat is largely observed in the northern Chukchi, East Siberian, and northern Laptev Seas (Figure 1a). The ice edge declined to some extent in the Kara and Barents Seas. The sea-ice decline recorded 4.71 million km^2 for September 2018, tying with 2008 for the 6th lowest September record in the last 40-year satellite periods (Figure 1b). The last five SIE lowest record for September i.e., before 2018, was observed during the year 2012 (1st), 2007 & 2016 (tied for 2nd lowest), 2011 (4th), and 2015 (5th), respectively [38] (Figure 2).

3.2. Warming impacts and reduction in Arctic sea-ice

The land-ocean temperature of Global (90ºS-90ºN) and Arctic (70 ºN+) regions are computed for the last 40 years (1979–2018). The average global air temperature has increased about 0.02 ± 0.02 °C year^{-1} (~0.78 °C in the last 40-year) while the Arctic air temperature has increased about 0.08 ± 0.02 °C year^{-1} (~3.1 °C in the last 40-year) (Figure 3a). However, to understand the influence of temperature in the Arctic region (70 ºN+), the air temperature data has been computed independently for the land and ocean for the last 40-year period (Figure 3b). The data analysis shows rapid warming trend in the Arctic ocean region (0.089 ± 0.01 °C year^{-1}; i.e., ~3.5 °C in the last 40-year) compared to the Arctic land region (0.072 ± 0.01 °C year^{-1}; i.e., ~2.8 °C in the last 40-year).

The four warmest years record (2016, 2017, 2018 and 2015) of the surface temperature have occurred in the past four years (Figure 4), and the top-ten warmest years are all observed in the past two decades (Figure 3). Two-thirds of global warming has occurred since 1979, at a rate of about 0.15–0.20 °C decade^{-1}. Advancement in Arctic warming is recorded since the year 2000, from all the months compared to the previous years. September 2018 was the 3rd warmest followed by 2016 and 2017 as 1st and 2nd warmest respectively (Figure 5). The AT over a great part of the Arctic Ocean was observed to be close to the normal. The conspicuous exemption being noticed in the East Siberian Sea, where

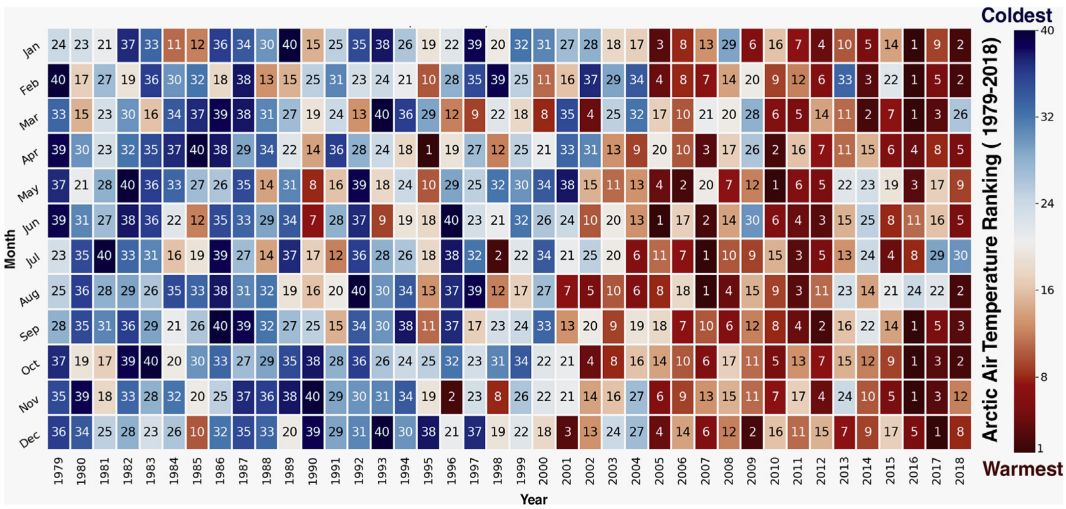

Figure 5. NCEP/NCAR Reanalysis air temperature at 925 hPa data of Artic region (70° N+) showing the monthly ranking (Jan to Dec) during the 1979–2018 period. The coldest months are illustrated using blue colour and warmest months using red colour. The map shows record warming, since the year 2000, in all the months compared to the previous years, while September 2018 was the 3rd warmest September in the satellite Era.

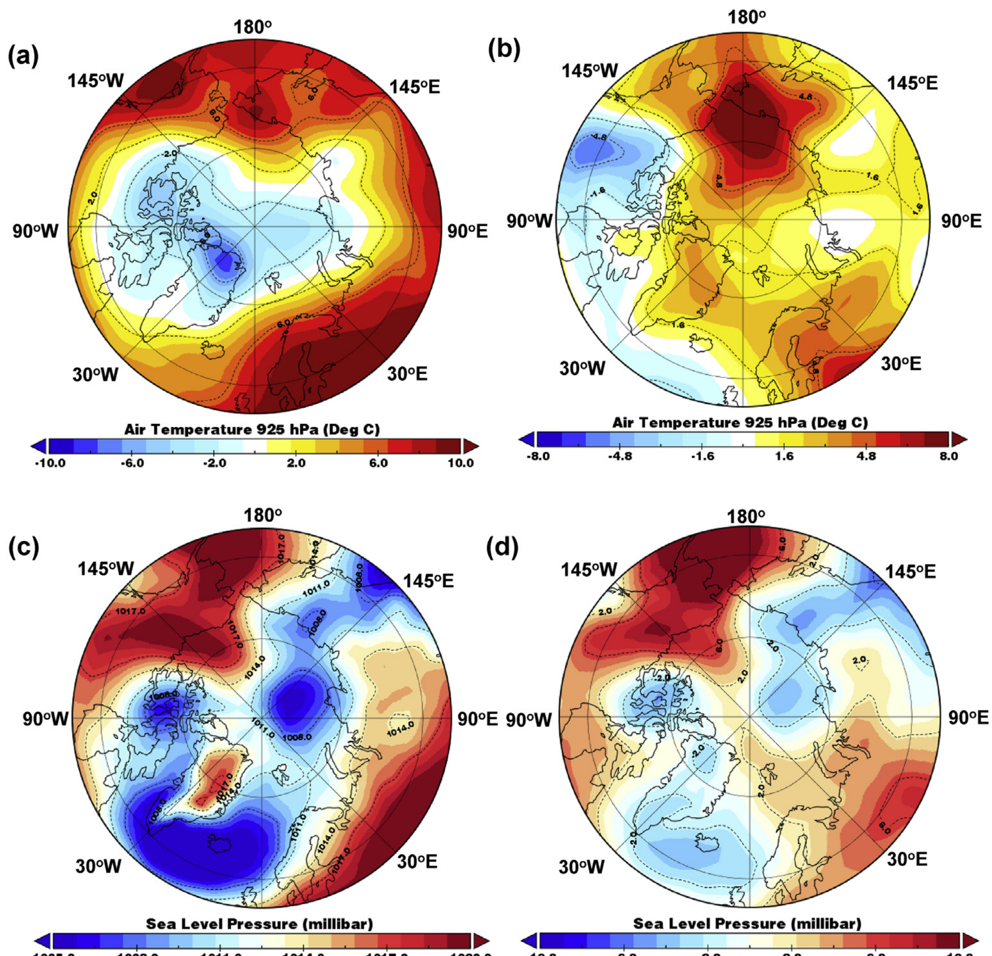

Figure 6. NCEP reanalysis derived data show the prevailing air temperature at 925 hPa (°C) and sea level pressure (mb) of September 2018 in the Arctic region. (a) Mean air temperature for the period of 1–19 September 2018; (b) Departure of a mean air temperature of 1–19 September 2018 from average air temperature of 1981–2010 in the Arctic (55°-90° N) at the 925 hPa level. Yellow to red colours indicates higher than the average air temperature and cyan to blue shows lower than the average air temperature. (c) SLP for the period of 1–19 September 2018; (d) Departure of SLP of 1–19 September 2018 from average SLP of 1981–2010 in the Arctic (55°-90° N). Red colour indicates higher than average SLP and blue colour indicates lower than average SLP.

temperatures were 7–9 °C above average for the first two weeks of September 2018 (Figure 6a, b). The average AT during July to September 2018 shows warming trends, whereas the higher temperatures were observed during September ranging from 3 to 8 °C above average over the western Beaufort, Chukchi, and East Siberian Seas induced due to a reduction in SIE (Figure 7). However, the mean SLP during these periods is dominated by a low-pressure area covering from the central Siberia, across the pole, and into the Canadian Arctic, and is most prominent, north of the Laptev Sea (Figures 6c, d and 7) which is linked to the decline in sea-ice.

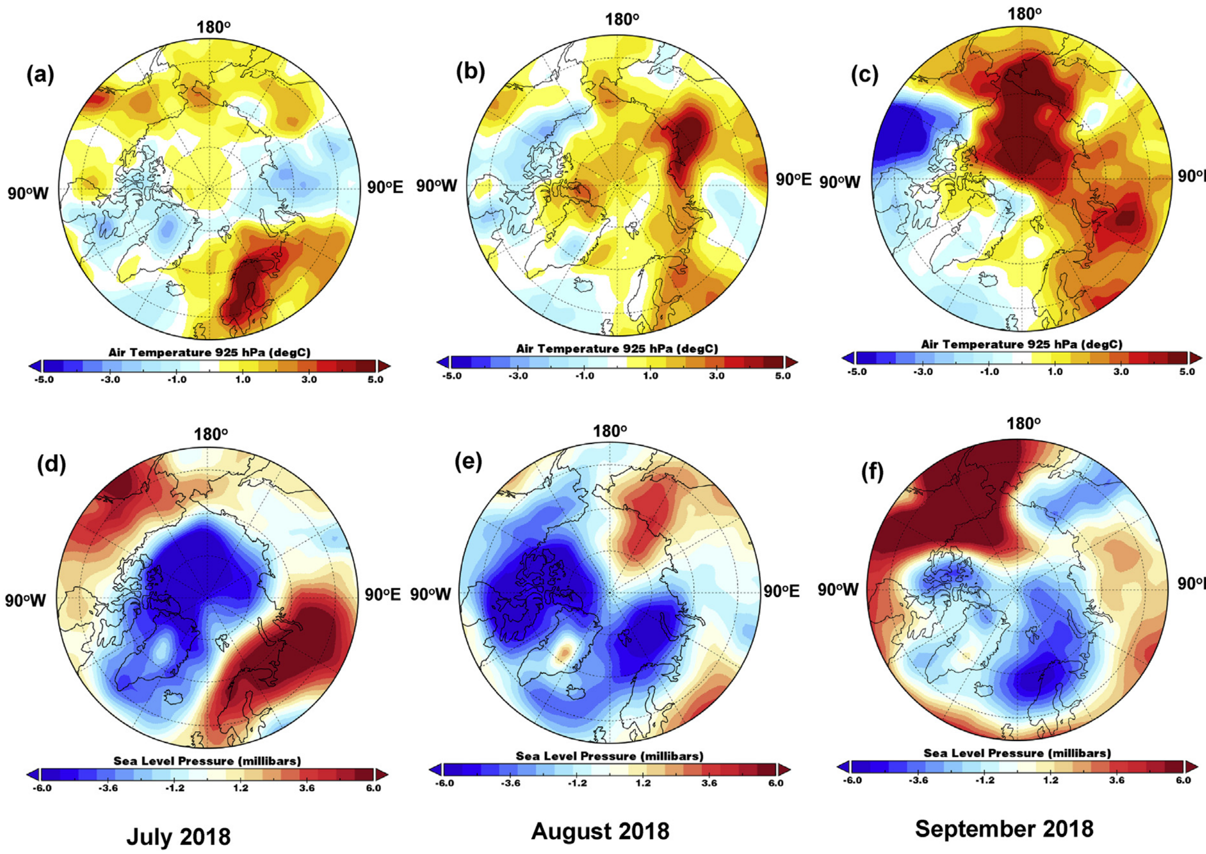

Figure 7. NCEP/NCAR reanalysis derived data show anomaly of AT (°C) and SLP (mb) in the Arctic region (55°-90° N) for the July, August, and September of 2018. (a–c) AT for July, August, and September, respectively, yellow to red colours indicates high temperature and cyan to blue show low temperature (d–f) SLP for July, August, and September, respectively, orange to red colour indicates high average SLP and cyan to blue colours indicate low SLP.

In the backdrop of global warming, the SIC in 2018 summer shows a rapid sea-ice decline from July to September (Figure 8a,b,c), since last four decades (1979–2018), Arctic SIE of September decreased by 12.8% decade^{-1} (Figure 1b). Sea-ice thickness (SIT) data for summer months of 2018 shows considerable thinning of sea-ice and it has been observed that approximately 80% of existing sea-ice is less than 1.5 m thick. However, SIT during peak summer (i.e., September 23, 2018) recorded maximum thinning (>80% area remains <1 m thick; Figure 8e). The unprecedented reduction in SIT is reported within the Arctic Ocean during all the summer months.

To understand the present status and reduction of SIT during summer 2018, sea-ice age data for the last 33-years [8, 34] were analyzed. Sea-ice age records show that the MYI extent has dramatically declined from 1984-2018 (Figure 9a). In September 2018, the MYI of +5-year, 4-year and 1-year has declined, except for 2–3 years its observed increase in SIE, compared to September 2017 (Figure 9a,b). During 2018, MYI covers 2 million km^{-2} and the oldest sea-ice, which remains at least four melt seasons covers about 1.5 million km^{-2}. The old sea-ice covered only 94,000 km^{-2} in 2018 at its lowest during September [38].

The accelerated decline of the Arctic ice over the past 40-year is showing alarming evidence of climate change (Figure 10). The sea-ice volume (SIV) is highly sensitive to climate change compared to SIE and SIT since it is declining at the highest rate. Based on the analysis of PIOMAS data, the Arctic SIV has declined more than half over the last four decades i.e., from 1979 to 2018, decreased 25,426 to 13,860 km^3, respectively at the rate of -3.0 ± 0.2 (1000 km^3 decade^{-1}). To understand the relation between Arctic warming and sea-ice decline, anomalies of SIE, SIV and AT show a remarkable relation between each other (Figure 10). An overall drastic decline in SIV is observed in the September month of the last 40-year – September 2018, which recorded three times lower than 1979 September (declined ~30% decade^{-1}). However, the year 2018 ended with an annually-averaged SIV (13,860 km^3) that was the 5th lowest on record, with a 1000 km^3 gain over the record year of 2017.

4. Discussion

4.1. Rapid decline in Arctic sea-ice linked to global warming

In recent decades, Arctic SIE has declined in all seasons since the year 1979–2018 (Figures 1 and 2) however, the accelerated decline was observed in the boreal summer (-10.2 ± 0.8 %decade^{-1}). The delay in the seasonal onset of ice growth may be due to shifting of the Arctic melt season at a rate of 5 days decade^{-1}. Additionally, the Arctic region is experiencing an imbalance due to the autumn sea ice growth that has been delayed by 6–11 days decade^{-1} within the eastern Beaufort Sea and the northern Kara and Barents Seas [40, 41]. The vertical mixing of the warm Atlantic water with the Kara Sea keeps the region warm that results in the delayed sea-ice retreat [42].

The temperature data analysis suggests progressive warming in the global scenario and the Arctic regions since the last two decades (Figure 3). The accelerated loss of sea-ice for the whole Arctic Ocean during September demonstrates that there are substantial variations in surface air temperature, and there is a correspondence between the fluctuations in surface air temperature in the Arctic and global regions (Figures 1 and 3). The warming rate in the Arctic recorded is faster than that of global temperature, a phenomenon often referred to as Arctic Amplification (AA). The phenomena of AA include a reduction in summer albedo (due to sea-ice and snow cover loss); the total water vapour increase; and the decrease (summer) and increase (winter) in total

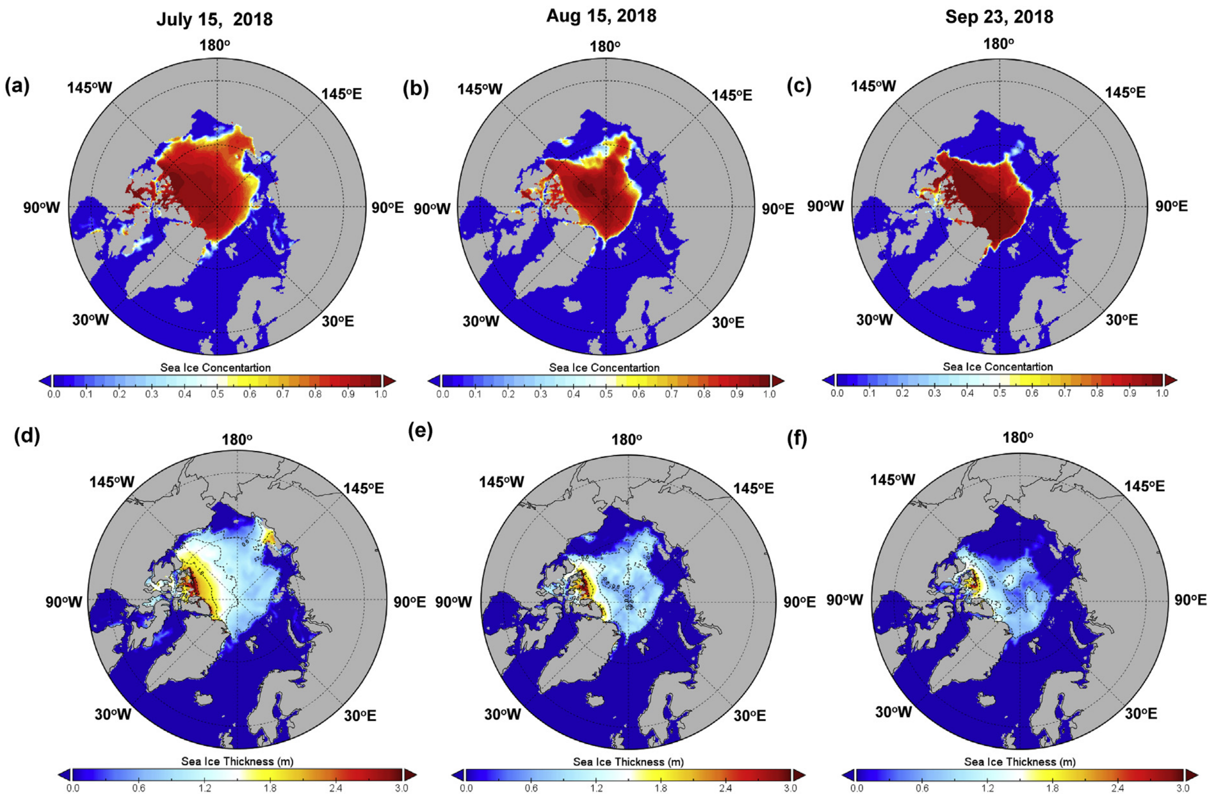

Figure 8. Daily SIC (ice in fraction) and SIT (m) for 2018 summer months (July–Sept) in the Arctic region. (a–c) Artic SIC on 15th July, 15th August and 23rd September of 2018; (d–f) Arctic SIT on 15th July, 15th August and 23rd September of 2018. The map illustrates the lowest SIC and SIT on 23rd September 2018.

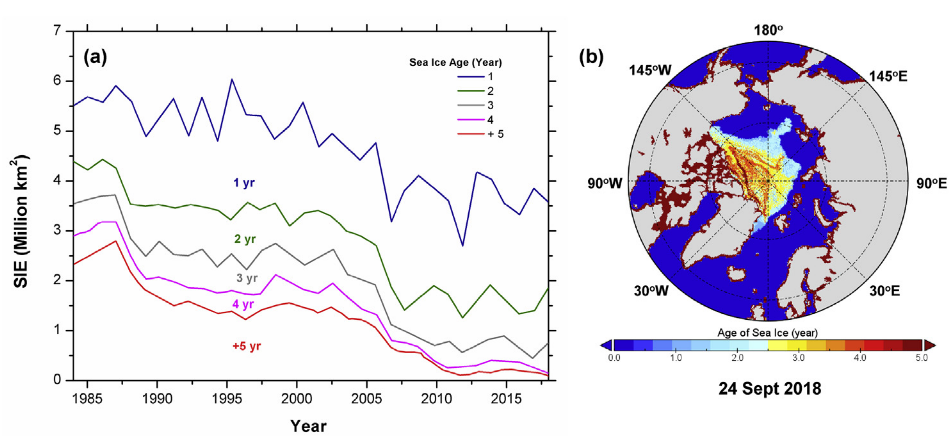

Figure 9. (a) Timeseries plot shows SIE of MYI at the end of each summer melt season (typically reached a minimum in September) since 1984–2018, sea ice age estimated using a Lagrangian tracking algorithm [8, 39]. The age of the ice is considered as first-year ice (0–1 years old), second-year ice (1–2 years old), and so forth based on how many summer melts seasons the ice packet remains [35]. (b) Ice age on September 24, 2018, shows the remaining sea ice age majorly ranging from 1-2 years only.

cloudiness [43]. The loss of Arctic sea-ice has emerged as an important signal of global warming [44, 45]. To identify large-scale oceanic factors linked to recent Global and Arctic warming, analysis of the supper El-Niño event (2014–2016) is explored (Figures 3 and 4). The ocean warming record shows the strong El Niño (2015–16) in the equatorial Pacific Ocean that is noticed in the annual mean surface temperature of 2015 than in 2016, but at the same time, the impact of El-Niño on global temperature was maximum in 2016 (Figure 4). It resulted in a lag of 3–4 months between El-Niños and their effect on global temperature. During 2018 annual mean surface temperature recorded the 3rd warmest year, the tropics having moved from the La-Niña phase to a weak El-Niño. NOAA forecasts a possibility of about 65% tropical warming, which may continue in the coming Northern Hemisphere spring and be classified as an El-Niño [46]. As a result, a large El Niño and an increase in the global temperature are observed in 2019 [47].

The month of July 2018 was the coldest (ranked as the 30th coldest July since 1979), especially over the East Siberian Sea and parts of the Kara Sea (Figures 5 and 7a), therefore could be attributable to the sea-ice retreat rate in the East Siberian Sea. However, AT in August 2018 (Figures 5 and 7b) was observed up to 5 °C above average in the Laptev Sea, despite the sea-ice loss (~57,500 km^2 day^{-1}) in August and was close to 1981 to 2010 average sea-ice loss. In the recent years (i.e., 2015–2018) the surface warming maxima were found in the Barents Sea, where the position of the sea-ice edge has been linked to variations in the inflow of Atlantic Water [24, 48]. A recent study suggests that the interaction between ocean heat transport and sea-ice influences mostly the shallow continental shelves [12].

Advancement in the Arctic warming has recorded the 3rd warmest September in 2018 since 1979 (Figure 5). The AT associated with the SLP (north of the Laptev Sea), in combination with the realm of a high-

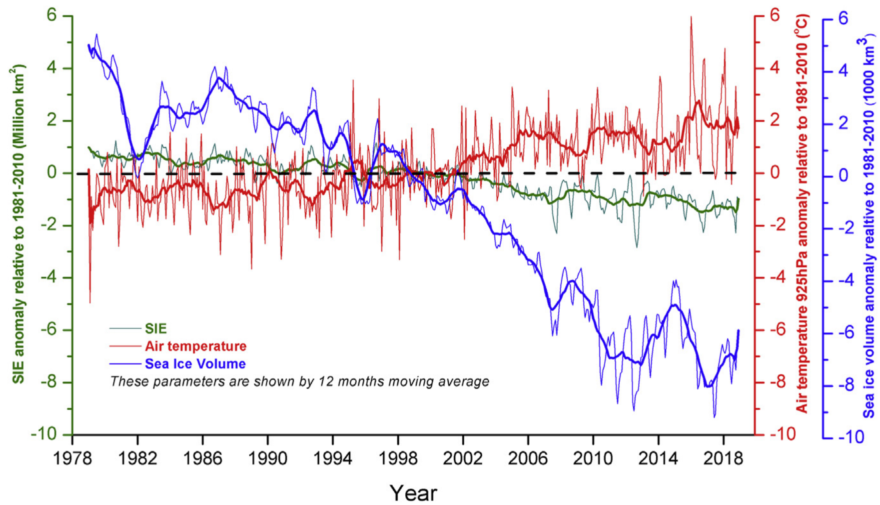

Figure 10. Monthly anomalies of SIE (million km^2), air temperature of NCEP/NCAR reanalysis at 925 hPa (°C) and sea ice volume (1000 km3) of PIOMAS, along with the annual running mean anomaly relative to 1981–2010. The SIE and sea ice volume have direct relation while air temperature demonstrates the inverse relationship.

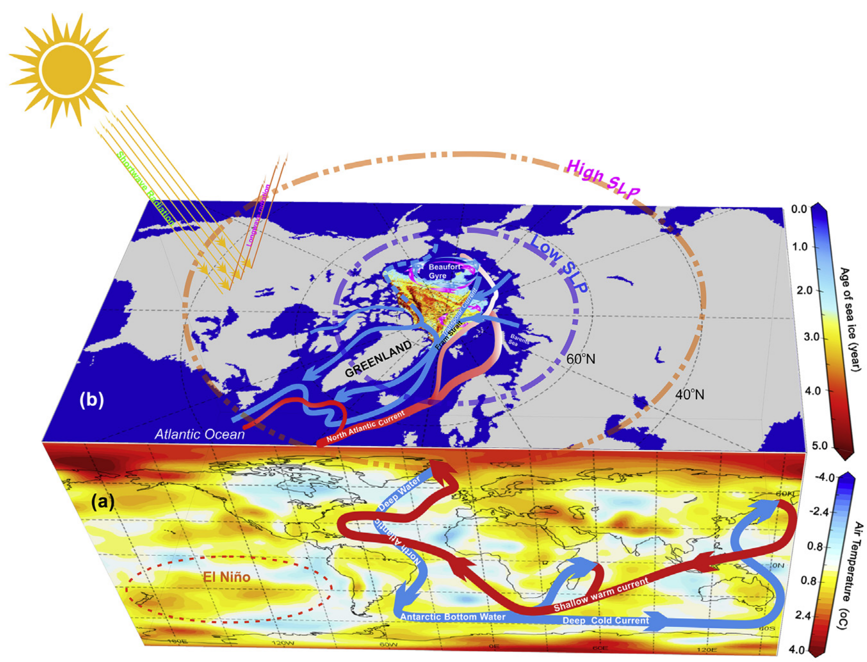

Figure 11. Schematic diagram illustrates the mechanism of the Arctic sea ice decline processes during 2018. The shortwave radiation enters in the Earth's atmosphere and the high solar energy absorbed by the surface, once heated up it re-emits longwave radiation with low energy [61]. (a) Shows the global air temperature anomaly for the year 2018 (3rd warmest year) relative to climatology using NCEP/NCAR reanalysis data. Warm surface currents are shown in red and cold deep ocean currents in blue that Illustrates the global thermohaline circulation system of the world ocean (after Richardson 2008) [62]. During 2018–2019, the tropics have moved from the La Niña phase to a weak El Niño, expected a large El Niño and increase in global temperature [46]. (b) The image illustrates the current system, substantially contributing to northward heat advection into the Arctic Ocean. The North Atlantic Current marked with red is warm, salty water and the blue arrows show cold, relatively fresh water. As an impact of land-ocean warming and formation of Beaufort Gyre, Arctic sea ice decline is accelerated and results in thinning of SIT and reduction in the existence of MYI for September 2018, oldest ice which has survived at least four melt seasons, covered only 94,000 km^{-2}. Dashed circle of red (blue) colour shows the region of high (low) SLP [46].

pressure ridge (at high altitudes, centred over the Bering Sea) was formed over the Bering Sea in early September [49] and drifted eastward, transported warm air from the south over the East Siberian Sea, helping to elucidate the high temperatures. The high-pressure ridge formed over the Bering Sea during early September, drifted eastward, which was observed late in the month, and further expanded into the Beaufort and Chukchi Seas (Figures 2 and 6). The high pressure contributed to slow freezing up of the water after the minimum sea-ice and warmed-up the region, where this high-pressure zone has formed. Alaska experienced its warmest period during September on record when sunny, warm, and dry conditions prevailed (Figure 7d). The loss of Arctic sea-ice is plausibly linked to the northward ocean heat transport, which results in the transfer of the warming signal from the Arctic to the tropics and thereby contracting the tropical circulation [50]. This melting is thereafter increased by positive feedbacks, viz the ice-albedo feedback, and enhances the shortwave absorption. The sea ice loss acts as a negative internal response in the tropical circulation to increased greenhouse gases [51]. The melting of Arctic sea-ice is thus an example of the robust responses to increased greenhouse gases and have major impacts on the hydrological circulation in the atmosphere [50].

4.2. Warming impacts and reduction in Arctic sea-ice

The SIE decrease in September 2018 is associated with a reduction of SIC in the surrounding Arctic regions, which has enhanced specifically in the East Siberian, Chukchi and Beaufort Seas (Figure 8c). Declining SIE and SIC are controlled by the ocean and atmospheric response [52]. The warm Atlantic water passes through the Fram Strait and the Barents Sea into the Arctic Ocean and dominates the ocean heat contribution to the Arctic Ocean [44] as shown in Figure 11. The decrease in SIE has been associated with major reductions in SIT (Figure 8d–f) that are primarily explained by variations in the ocean's coverage of multiyear ice (MYI) [8, 53]. Reconstructed SIT measurements in the central Arctic showed a decline of about 65 % since the mid-1970s [22]. The recent study suggests that seasonal ice has largely replaced MYI as the dominant form of ice, and has the potential to promote a gradual shift to a seasonally ice-free Arctic state [16]. Accelerated decline in the amount of MYI that persisted at the end of summer is found to be considerably lower than that of the 1980s and 1990s MYI (Figure 9a). The earlier study revealed that the MYI of total winter ice extent from the mid-1980s to 2018 decreased by about 25% [23]. The land-ocean warming and formation of the Beaufort Gyre [54] have intensified the loss of sea ice by thinning of SIT and the MYI reduction in September 2018 (Figure 11). The Arctic Ocean has lost about 3/4 of the sea-ice volume in the last four decades, which corresponds to an average reduction of SIE and SIT by half, at the end of the summer season [55]. The global warming effect shows a possible impact of Arctic sea-ice loss on tropical regions [56], which has some teleconnections and relationships with various global phenomena-Arctic Oscillation, Hadley circulation, North Atlantic Oscillation and Asian Summer Monsoon rainfall-and tropical climate processes [57, 58, 59]. The accelerated decline in sea-ice is associated with the weakening of the polar cell and an inconsistent increase in SLP over high latitude (60°N), along with the Urals–Siberia and Iceland low regions (Figures 6 and 7), whereas, it is also connected to the weakening of the three-cell circulations and a warmer SST in the midlatitude North Atlantic [60].

5. Summary and conclusions

In the last 40 years, the Arctic SIE has declined significantly (at the rate of $-55398 \pm 3113\ km^2\ year^{-1}$) and the rate of decline was maximum in the boreal summer months especially in each September. The SIE on September 23, 2018, was the sixth-lowest record (~1.70 million km^2 below from the 30-year climatology) and it retreated largely in the northern Chukchi, East Siberian, northern Laptev Seas and to some extent in the Kara and Barents Seas (Figures 1 and 8). The warming over the western Beaufort, Chukchi, and East Siberian Seas (3–8 °C above average) region and the low-pressure area extending from central Siberia, Canadian Arctic, and north of the Laptev Sea induced to reduce the SIE.

Study reveals SIE minimum and the warmest September records occurred in the last twelve years of the satellite era. During the 40 years (1979–2018), the average AT of the Arctic has increased four-times higher than the global AT, which resulted in AA and is linked to the northward heat advection into the Arctic Ocean. However, the recent SIE and SIC decline are also influenced by the El- Niño in the equatorial Pacific Ocean. In summer 2018, we find a considerable decline in the amount of MYI and thinning in SIT primarily over Eurasia and the central Arctic. During spring and summer - over the last four decades, the MYI moved into the Beaufort Sea from the northwest and declined half of its SIV. This melting and sea-level rise are greater than predicted [63], however, there is no record of such a sea-level rise. To understand the mechanism associated with the sea-ice decline a schematic diagram is shown in Figure 11. Further, the study would be required to evaluate the amount of sea-ice melting with an influence of warm ocean water intrusions in high latitudes.

Declarations

Author contribution statement

A. Kumar: Conceived and designed the experiments; Analyzed and interpreted the data; Wrote the paper.

J. Yadav: Analyzed and interpreted the data; Contributed reagents, materials, analysis tools or data; Wrote the paper.

R. Mohan: Conceived and designed the experiments; Wrote the paper.

Funding statement

This research did not receive any specific grant from funding agencies in the public, commercial, or not-for-profit sectors.

Competing interest statement

The authors declare no conflict of interest.

Additional information

No additional information is available for this paper.

Acknowledgements

We gratefully acknowledge Dr. M. Ravichandran, Director, National Centre for Polar and Ocean Research (NCPOR), Goa and Ministry of Earth Sciences (MoES), New Delhi, for continuous support and encouragement. Juhi Yadav thanks the University Grants Commission (UGC), New Delhi, India, for the award of Junior Research Fellowship [No. F.15-6(DEC.2018)/2019(NET)]. The authors sincerely acknowledge various organisations such as National Snow and Ice Data Center (NSIDC), National Oceanic and Atmospheric Administration (NOAA), Copernicus Marine Environment Monitoring Service, National Centre for Atmospheric Research (NCAR), Technische Universitat Dresden, and the Polar Science Center, Applied Physics Laboratory for making various datasets available in their portals. Authors thank anonymous reviewers and Editor - Earth Science, for their insightful comments and suggestions on the previous draft, which improved the quality of the paper. This is NCPOR contribution no J-14/2020–21.

References

[1] M.C. Serreze, J.A. Maslanik, T.A. Scambos, F. Fetterer, J. Stroeve, K. Knowles, C. Fowler, S. Drobot, R.G. Barry, T.M. Haran, A record minimum arctic sea ice extent and area in 2002, Geophys. Res. Lett. 30 (2003) 1–4.
[2] J.C. Stroeve, T. Markus, L. Boisvert, J. Miller, A. Barrett, Changes in Arctic melt season and implications for sea ice loss, Geophys. Res. Lett. 41 (2014) 1216–1225.
[3] J. Stroeve, D. Notz, Changing state of Arctic sea ice across all seasons Changing state of Arctic sea ice across all seasons, Environ. Res. Lett. 13 (2018) 103001.
[4] C.L. Parkinson, D.J. Cavalieri, Arctic sea ice variability and trends, 1979–2006, J. Geophys. Res. Ocean. 113 (2008) 1–19.
[5] M.C. Serreze, A.P. Barrett, A.G. Slater, M. Steele, J. Zhang, K.E. Trenberth, The large-scale energy budget of the Arctic, J. Geophys. Res. 112 (2007) D11122.
[6] J.C. Comiso, C.L. Parkinson, Arctic sea ice parameters from AMSR-E data using two techniques and comparisons with sea ice from SSM/I, J. Geophys. Res. 113 (2008) C02S05.
[7] A. Morrow, Arctic Sea Ice Wintertime Extent Hits Another Record Low, 2016. Http://Www.Nasa.Gov/. http://www.nasa.gov/feature/goddard/2016/2016-arctic-sea-ice-wintertime-extent-hits-another-record-low#.V08CEqFznbI.mendeley.
[8] J. Maslanik, J. Stroeve, C. Fowler, W. Emery, Distribution and trends in Arctic sea ice age through spring 2011, Geophys. Res. Lett. 38 (2011) n/a-n/a.
[9] R. Kwok, J.C. Comiso, S. Martin, R. Drucker, Ross sea polynyas : response of ice concentration retrievals to large areas of thin ice 112 (2007) 1–13.
[10] J.C. Stroeve, Arctic sea ice plummets in 2007, Trans. Am. Geophys. Union 89 (2008) 13–14.
[11] J.C. Comiso, F. Nishio, Trends in the sea ice cover using enhanced and compatible AMSR-E, SSM/I, and SMMR data, J. Geophys. Res. 113 (2008) C02S07.
[12] G. Auclair, L.B. Tremblay, The role of ocean heat transport in rapid sea ice declines in the community Earth system model large ensemble, J. Geophys. Res. Ocean. 123 (2018), 2018JC014525.
[13] R. Kwok, E.C. Hunke, W. Maslowski, D. Menemenlis, J. Zhang, Variability of sea ice simulations assessed with RGPS kinematics, J. Geophys. Res. 113 (2008) C11012.
[14] J.A. Francis, The Arctic matters: extreme weather responds to diminished Arctic Sea ice, Environ. Res. Lett. 10 (2015), 091002.
[15] E. Carmack, I. Polyakov, L. Padman, I. Fer, E. Hunke, J. Hutchings, J. Jackson, D. Kelley, R. Kwok, C. Layton, H. Melling, D. Perovich, O. Persson, B. Ruddick, M.-L. Timmermans, J. Toole, T. Ross, S. Vavrus, P. Winsor, E. Carmack, I. Polyakov, L. Padman, I. Fer, E. Hunke, J. Hutchings, J. Jackson, D. Kelley, R. Kwok, C. Layton, H. Melling, D. Perovich, O. Persson, B. Ruddick, M.-L. Timmermans, J. Toole, T. Ross, S. Vavrus, P. Winsor, Toward quantifying the increasing role of oceanic heat in sea ice loss in the New arctic, Bull. Am. Meteorol. Soc. 96 (2015) 2079–2105.
[16] M.M. Holland, C.M. Bitz, B. Tremblay, Future abrupt reductions in the summer Arctic sea ice, Geophys. Res. Lett. 33 (2006) 1–5.
[17] J. Huang, X. Zhang, Q. Zhang, Y. Lin, M. Hao, Y. Luo, Z. Zhao, Y. Yao, X. Chen, L. Wang, S. Nie, Y. Yin, Y. Xu, J. Zhang, Recently amplified arctic warming has contributed to a continual global warming trend, Nat. Clim. Change 7 (2017) 875–879.
[18] M. Ogi, K. Yamazaki, J.M. Wallace, Influence of winter and summer surface wind anomalies on summer Arctic sea ice extent, Geophys. Res. Lett. 37 (2010) 1–5.

[19] M. Ogi, J.M. Wallace, Summer minimum Arctic sea ice extent and the associated summer atmospheric circulation, Geophys. Res. Lett. 34 (2007) L12705.
[20] A.C. Bliss, M. Steele, G. Peng, W.N. Meier, S. Dickinson, Regional variability of Arctic sea ice seasonal change climate indicators from a passive microwave climate data record, Environ. Res. Lett. (2019).
[21] C.L. Parkinson, D.J. Cavalieri, Antarctic Sea Ice Variability and Trends, 1979–2010, 2012.
[22] R. Lindsay, A. Schweiger, Arctic sea ice thickness loss determined using subsurface, aircraft, and satellite observations, Cryosphere 9 (2015) 269–283.
[23] R. Kwok, Arctic sea ice thickness, volume, and multiyear ice coverage: losses and coupled variability (1958–2018), Environ. Res. Lett. 13 (2018) 105005.
[24] I.H. Onarheim, T. Eldevik, L.H. Smedsrud, J.C. Stroeve, I.H. Onarheim, T. Eldevik, L.H. Smedsrud, J.C. Stroeve, Seasonal and regional manifestation of Arctic sea ice loss, J. Clim. 31 (2018) 4917–4932.
[25] N.C. Swart, J.C. Fyfe, E. Hawkins, J.E. Kay, A. Jahn, Influence of internal variability on Arctic sea-ice trends, Nat. Clim. Change 5 (2015) 86–89.
[26] D.J. Cavalieri, C.L. Parkinson, P. Gloersen, H.J. Zwally, Sea Ice Concentrations from Nimbus-7 SMMR and DMSP SSM/I-SSMIS Passive Microwave Data, Version 1 [daily, Arctic Ocean, 1978–2015], Natl. Snow Ice Data Center, 1996. Boulder, Color. USA. updated yearly.
[27] F. Fetterer, K. Knowles, W.N. Meier, M. Savoie, A.K. Windnagel, Sea Ice Index, Version 3. (Arctic, Updated Daily), NSIDC: National Snow and Ice Data Center, Boulder, Colorado USA, 2017.
[28] D.J. Cavalieri, C.L. Parkinson, Arctic sea ice variability and trends, 1979–2010, Cryosphere 6 (2012) 881–889.
[29] E. Kalnay, M. Kanamitsu, R. Kistler, W. Collins, D. Deaven, L. Gandin, M. Iredell, S. Saha, G. White, J. Woollen, Y. Zhu, M. Chelliah, W. Ebisuzaki, W. Higgins, J. Janowiak, K.C. Mo, C. Ropelewski, J. Wang, A. Leetmaa, R. Reynolds, R. Jenne, D. Joseph, The NCEP/NCAR 40-year reanalysis project, Bull. Am. Meteorol. Soc. 77 (1996) 437–471, 2.
[30] M.C. Serreze, J. Stroeve, Arctic sea ice trends, variability and implications for seasonal ice forecasting, Philos. Trans. A. Math. Phys. Eng. Sci. 373 (2015).
[31] H.J. Zwally, B. Schutz, W. Abdalati, J. Abshire, C. Bentley, A. Brenner, J. Bufton, J. Dezio, D. Hancock, D. Harding, T. Herring, B. Minster, K. Quinn, S. Palm, J. Spinhirne, R. Thomas, ICESat's laser measurements of polar ice, atmosphere, ocean, and land, J. Geodyn. 34 (2002) 405–445.
[32] R. Bleck, An oceanic general circulation model framed in hybrid isopycnic-Cartesian coordinates, Ocean Model. (2002).
[33] P. Sakov, F. Counillon, L. Bertino, K.A. Lisæter, P.R. Oke, A. Korablev, TOPAZ4: an ocean-sea ice data assimilation system for the North Atlantic and Arctic, Ocean Sci. 8 (2012) 633–656.
[34] M.A. Tschudi, W.N. Meier, J.S. Stewart, An enhancement to sea ice motion and age products, Cryosphere Discuss. (2019) 1–29.
[35] M. Tschudi, C. Fowler, J. Maslanik, J. Stroeve, Tracking the movement and changing surface characteristics of Arctic sea ice, IEEE J. Sel. Top. Appl. Earth Obs. Remote Sens. 3 (2010) 536–540.
[36] A. Schweiger, R. Lindsay, J. Zhang, M. Steele, H. Stern, R. Kwok, Uncertainty in modeled Arctic sea ice volume, J. Geophys. Res. 116 (2011) C00D06.
[37] J. Zhang, D.A. Rothrock, Modeling global sea ice with a thickness and enthalpy distribution model in generalized curvilinear coordinates, Mon. Weather Rev. 131 (2003) 845–861.
[38] NSIDC, Arctic summer 2018: September extent ties for sixth lowest, Arct. Sea Ice News Anal. (2018). http://nsidc.org/arcticseaicenews/2018/10/september-extent-ties-for-sixth-lowest/ (Accessed March 17, 2019).
[39] M. Tschudi, W.N. Meier, J.S. Stewart, C. Fowler, J. Maslanik, EASE-Grid Sea ice age, Version 4. [Arctic], boulder, color. USA. NASA Natl. Snow ice data cent, Distrib. Act. Arch. Center. (2019).
[40] J.C. Stroeve, T. Markus, L. Boisvert, J. Miller, A. Barrett, Changes in Arctic melt season and implications for sea ice loss, Geophys. Res. Lett. (2014).
[41] G. Peng, M. Steele, A.C. Bliss, W.N. Meier, S. Dickinson, G. Peng, M. Steele, A.C. Bliss, W.N. Meier, S. Dickinson, Temporal means and variability of Arctic sea ice melt and freeze season climate indicators using a satellite climate data record, Rem. Sens. 10 (2018) 1328, 10 (2018) 1328.
[42] R.C. Boeke, P.C. Taylor, Seasonal energy exchange in sea ice retreat regions contributes to differences in projected Arctic warming, Nat. Commun. 9 (2018) 1–14.
[43] J.T.M. Lenaerts, K. Van Tricht, S. Lhermitte, T.S. L'Ecuyer, Polar clouds and radiation in satellite observations, reanalyses, and climate models, Geophys. Res. Lett. 44 (2017) 3355–3364.
[44] M. Muilwijk, L.H. Smedsrud, M. Ilicak, H. Drange, Atlantic water heat transport variability in the 20th century Arctic ocean from a global Ocean Model and observations, J. Geophys. Res. Ocean. 123 (2018) 8159–8179.
[45] J. Yadav, A. Kumar, R. Mohan, Dramatic decline of Arctic sea ice linked to global warming, Nat. Hazards (2020).
[46] J. Hansen, M. Sato, R. Ruedy, G.A. Schmidt, K. Lo, Global Temperature in 2018 and beyond, 2019. http://data.giss.nasa.gov/gistemp/. (Accessed 18 March 2019).
[47] L. Cheng, J. Abraham, J. Zhu, K.E. Trenberth, J. Fasullo, T. Boyer, R. Locarnini, B. Zhang, F. Yu, L. Wan, X. Chen, X. Song, Y. Liu, M.E. Mann, Record-setting ocean warmth continued in 2019, Adv. Atmos. Sci. 37 (2020) 137–142.
[48] I.H. Onarheim, M. Årthun, Toward an ice-free Barents Sea, Geophys. Res. Lett. 44 (2017) 8387–8395.
[49] J. Samenow, A massive, historic high-pressure zone is bringing freakishly nice weather to Alaska, Cap, Weather Gang Rep, The Washingt, 2018. Post, https://www.washingtonpost.com/weather/2018/10/02/massive-historic-high-pressure-zone-is-bringing-freakishly-nice-weather-alaska/?noredirect=on&utm_term=.21910bb6341f.
[50] R. Chemke, L.M. Polvani, C. Deser, The effect of Arctic sea ice loss on the Hadley circulation, Geophys. Res. Lett. 46 (2019) 963–972.
[51] R. Chemke, L.M. Polvani, Ocean circulation reduces the Hadley cell response to increased greenhouse gases, Geophys. Res. Lett. 45 (2018) 9197–9205.
[52] Z. Labe, Y. Peings, G. Magnusdottir, Contributions of ice thickness to the atmospheric response from projected Arctic sea ice loss, Geophys. Res. Lett. 45 (2018) 5635–5642.
[53] R. Kwok, G.F. Cunningham, M. Wensnahan, I. Rigor, H.J. Zwally, D. Yi, Thinning and volume loss of the Arctic Ocean sea ice cover: 2003–2008, J. Geophys. Res. 114 (2009) C07005.
[54] A.C. Bliss, M.R. Anderson, Arctic sea ice melt onset timing from passive microwave-based and surface air temperature-based methods, J. Geophys. Res. Atmos. (2018).
[55] J.-C. Gascard, J. Zhang, M. Rafizadeh, Rapid Decline of Arctic Sea Ice Volume: Causes and Consequences, 2019.
[56] P.-A. Monerie, T. Oudar, E. Sanchez-Gomez, Respective impacts of Arctic sea ice decline and increasing greenhouse gases concentration on Sahel precipitation, Clim. Dynam. (2018) 1–18.
[57] F. Li, H. Wang, J. Liu, The strengthening relationship between Arctic Oscillation and ENSO after the mid-1990s, Int. J. Climatol. 34 (2014) 2515–2521.
[58] A. Prabhu, P.N. Mahajan, R.M. Khaladkar, Association of the Indian summer monsoon rainfall variability with the geophysical parameters over the Arctic region, Int. J. Climatol. Int. J. Clim. 32 (2012) 2042–2050.
[59] F. Li, Q. Zeng, Statistical prediction of East Asian summer monsoon rainfall based on SST and sea ice concentration, J. Meteorol. Soc. Japan. Ser. II. 86 (2008) 237–243.
[60] H.H.N. Cheung, N. Keenlyside, N.-E. Omrani, W. Zhou, N. Keenlyside, N.-E. Omrani, W. Zhou, Remarkable link between projected uncertainties of Arctic sea-ice decline and winter eurasian climate, Adv. Atmos. Sci. 35 (2018) 38–51.
[61] A. Donohoe, K.C. Armour, A.G. Pendergrass, D.S. Battisti, Shortwave and longwave radiative contributions to global warming under increasing CO2, Proc. Natl. Acad. Sci. U. S. A. 111 (2014) 16700–16705.
[62] P.L. Richardson, On the history of meridional overturning circulation schematic diagrams Progress in Oceanography, Prog. Oceanogr. 76 (2008) 466–486.
[63] A.A. Khan, Why would sea-level rise for global warming and polar ice-melt? Geosci. Front. 10 (2019) 481–494.